E-466
FERMILAB-PUB-80-116-E
Submitted to
Phys. Rev. C.

# Test of the applicability of the two-step model to the emmission of Sc fragments in the interaction of $^{238}U$ with 400 GeV protons



D. R. Fortney* and N. T. Porile

Department of Chemistry, Purdue University,

W. Lafayette, Indiana 47907

Differential ranges of $^{44}Sc^{m}$, $^{46}Sc$, $^{47}Sc$, and $^{48}Sc$ emitted at 17° and 163° to the beam in the interaction of $^{238}U$ with 400 GeV protons have been measured. The mean kinetic energies of the fragments decrease from 54.2 ± 1.0 MeV at 17° to 42.0 ± 0.7 MeV at 163°. From this shift, the mean velocity of the emitting nucleus $\langle v_{||} \rangle$ is obtained as 0.10 $(MeV/A)^{1/2}$. The angular distribution of Sc fragments in a system moving with this velocity is found to be asymmetric about 90° with more fragments emitted at backward than at forward angles (F/B ∿ 0.8). The implications of this result for the reaction mechanism are considered.

NUCLEAR REACTIONS $^{238}U(p,x)$ $^{44}Sc^{m}$, $^{46}Sc$, $^{47}Sc$, $^{48}Sc$; $T_p$ = 400 GeV. Measured differential ranges at 17° and 163°; deduced two-step model parameters.

*Present address: Sandia Corporation, Albuquerque, New Mexico

## I. Introduction

The study of highly inelastic interactions of multi-GeV protons with heavy elements has revealed a number of features that were totally unexpected on the basis of results obtained at lower energies. Beg and Porile[1] thus discovered that the ratio of forward-to-backward emission (F/B) of various deep spallation products of the interaction of $^{238}U$ with protons peaked rather sharply at 3 GeV while the ranges decreased abruptly between 1 and 5 GeV. Similar results were subsequently reported for a number of other deep spallation and fragmentation products of the interaction of uranium and gold with high-energy protons.[2-5] More detailed differential range measurements have shown that, in addition to a decrease in the mean range, a substantial broadening of the distributions occurs.[6,7] The angular distributions of the products in question also undergo a remarkable change. At energies of 3 GeV and below the differential cross sections thus peak at forward angles[8-11] while at 11.5 GeV and above sideward peaking is observed.[6,10-14]

The results obtained at high energies appear to be inconsistent with the conventional two-step mechanism in which a prompt intranuclear cascade initiated by the incident proton is followed by a slow deexcitation process such as evaporation or two-body breakup. According to this model, the products of these highly inelastic interactions require the transfer of large amounts of excitation energy and momentum to the struck nucleus and their angular distributions should thus peak at forward angles.[4,5] It appears, instead, that near-central interactions at high energies may be understood in terms of the coherent interaction model[16] and a number of qualitative and quantitative applications of this model to the results of present interest have recently been made.[5,17,18] The following picture emerges

from these considerations: Viewed in the projectile frame, the target nucleus is longitudinally Lorentz contracted. As a result, the incident proton interacts coherently with an imaginary tube comprised of all the nucleons lying in its path. Because of relativistic time dilation, the tube is ejected from the nucleus prior to decay to the final multi-particle state. Frictional effects and final state interactions may lead to additional mass loss from the region adjacent to the ejected tube. The spectator remnant is highly unstable and rapidly breaks apart in the transverse direction giving rise to fragments and deep spallation products having the properties described above.

Recent angular distribution measurements on products from the interaction of $^{238}U$ with 400 GeV protons indicate that while sideward peaking is even more pronounced than it is at 11.5 GeV, a new feature may be noted at this energy.[11,13] Emission at backward angles is thus found to be more probable than that at the corresponding forward angles. This novel feature appears to be most pronounced for products in the A = 40-50 mass region, i.e. Sc fragments, but is also observed for neutron deficient nuclides as massive as $^{106}Ag^{m}$. By contrast, the angular distributions of Sc fragments at 11.5 GeV had been found to be essentially symmetric about 90° to the beam in the laboratory system.[10,11] While these results indicate the occurrence of a new phenomenon at ultra-high energies, they are not sufficiently detailed to permit a unique explanation. The effect in question could thus result from an unusual kind of two-step process in which the struck nucleus recoils backward in the laboratory system and then breaks up symmetrically in the moving frame. On the other hand,

the results could also be explained as resulting from the asymmetric breakup of a nucleus moving along the beam direction. Intermediate cases are, of course, also possible. The angular distribution simply does not place enough constraints on the kinematics to permit a choice between the different possibilities.

Cumming and coworkers[8,9,19] have shown that the determination of differential ranges at various angles to the beam provides the information for a more definitive interpretation of the angular distribution. Mean fragment velocities may be derived from these data. The difference in the mean velocity of fragments emitted along and opposite to the beam permits a determination of the mean velocity of the moving system. The laboratory angular distributions may be transformed to this system and examined for symmetry. A symmetric angular distribution is taken as evidence that the impact (e.g. intranuclear cascade, coherent interaction) and breakup (e.g. two-body breakup, evaporation) steps are temporally well separated so that the reaction can be satisfactorily described by a two-step model. On the other hand, an asymmetric angular distribution indicates that when breakup occurs the nucleus still retains a memory of the beam direction. In this case, the reaction does not involve two well separated steps. In the first experiment of this type[8] it was thus shown that the formation of $^{24}Na$ in the interaction of $^{209}Bi$ with 2.9 GeV protons could not be described by a two-step model as the angular distribution in the moving system was forward-peaked. This result was subsequently confirmed by on-line counter measurements of the double differential cross sections for the emission of light fragments in the interaction of $^{238}U$ with $\sim$ 5 GeV protons.[20,21] Similar experiments performed on $^{131}Ba$ from $^{238}U$ plus 2.2 GeV protons,[9] $^{149}Tb$ from $^{197}Au$ plus 2.2 GeV protons,[19] and $^{24}Na$ from $^{197}Au$ plus 11.5 GeV protons[14] indicated, on the other hand, that the data were consistent with the two-step model.

In previous publications from this laboratory we have reported the angular distributions of $^{44}Sc^{m}$, $^{46}Sc$, $^{47}Sc$, and $^{48}Sc$ emitted in the interaction of $^{238}U$ with 400 GeV protons[11,13] as well as the differential ranges of these fragments at 90° to the beam.[7] We present here the results of differential range measurements on Sc fragments emitted at forward and backward angles. When combined with our previously reported results, these data permit a detailed kinematic analysis to test the applicability of the two-step model.

## II. Experimental

The experimental procedure has been described in detail in a previous report.[7] Briefly, thin $UF_4$ targets (~ 200μg/cm$^2$) evaporated onto pure aluminum were exposed to a 400 GeV proton beam in an evacuated chamber at Fermilab. The targets were oriented at 90° to the beam. Fragments recoiling out of the target at angles of either 6° - 25° or 155° - 174° to the beam were caught in stacks of thin (300-400 μg/cm$^2$) Mylar foils. The angular range was defined by a thick aluminum mask whose opening was cut along isotheta lines.[22,23] A code described elsewhere[23] was used to determine the mean recoil angle and the solid angle subtended by the catchers, as well as to evaluate the correction to the target and catcher thickness resulting from the dispersion in fragment path length due to the large catcher width. The mean recoil angles were either 17° or 163°

Following irradiation, scandium was separated from the catcher foils and the γ-ray activity of the samples assayed with Ge(Li) spectrometers. The differential ranges were obtained from the measured counting rates

after extrapolation to end of bombardment and correction for chemical yield, variation in catcher thickness, and path length dispersion.

## III. Results and Discussion

### A. Differential ranges and energy spectra

The results of one of two replicate experiments performed at each angle are shown as histograms in Fig. 1. The results of our previously reported[7] measurements on Sc fragments emitted at 90° (80° - 100°) are included for completeness. The indicated uncertainties were obtained by combining those in the Mylar foil thickness and uniformity (3%), chemical yield determination (2%), and correction for path length dispersion (1%) with the statistical uncertainty. The overall uncertainties typically ranged from ∿ 4% near the peak of the differential range to ∿ 50% for the last foil showing activity above background, except for $^{46}$Sc whose long half-life led to larger statistical errors. A small resolution correction was applied to the differential ranges in the manner described elsewhere.[7]

The corrected differential ranges were curve-fitted by use of a non-linear regression analysis code as described in our previous report.[7] The purpose of this procedure was to facilitate the combination of replicate results as well as the transformation from range to energy spectra. The results of this procedure are shown as the curves in Fig. 1. Note that these curves generally do not pass through the midpoints of the histograms but through the effective midpoints obtained by application of the resolution correction, the difference being most noticeable in the steepest regions of the curves.

The differential ranges were converted to energy spectra by use of the range-energy table of Northcliffe and Schilling.[24] A small correction, amounting to <1% for all but the lowest energy fragments, was applied to account for the difference between the tabulated[24] path lengths and the experimentally determined projected ranges. The magnitude of this correction was obtained from the theory of Lindhard, Scharff, and Schiøtt.[25] A further correction was applied to the data in order to account for the energy loss of the fragments in the $UF_4$ target. It was assumed that, on the average, the fragments traversed half the corrected target thickness and the range-energy table[24] was used to compute this additional energy loss. It was found that energy loss in the target ranged from ∿ 5% for the lowest energy fragments to ∿ 1% for those of highest energy. The effective target thickness corresponds to ∿ 40 $\mu g/cm^2$ Mylar. The spectra obtained in this fashion for $^{44}Sc^m$ and $^{47}Sc$ are displayed in Figs. 2 and 3, respectively. The points represent the transformed corrected differential ranges obtained in replicate experiments. The error bars incorporate an estimated 5% uncertainty in the range-energy relation. The curves were obtained from the corresponding fitted range curves generated with the average values of the fitting parameters obtained in the replicate runs. It is seen that the curves generally represent an excellent fit to the data points. The spectra obtained for $^{46}Sc$ and $^{48}Sc$ are very similar to the corresponding $^{47}Sc$ or $^{44}Sc^m$ spectra.

The mean fragment energies are listed in Table I. Our previous[7] 90° results are included for completeness. The tabulated errors are the larger of the standard deviations and the estimated uncertainties in the individual determinations. The uncertainty in the range-energy relation is not included

in this estimate since it does not affect the variation of the energies with angle. Since there appears to be little, if any, systematic difference between the various Sc fragments, the uncertainties can be further reduced by evaluation of a weighted average. This quantity is included in the table. Since, for the purposes of a vector-model analysis, the fragment velocities are more useful than the energies, velocity spectra were directly obtained from the differential ranges. The mean fragment velocities as well as the widths (full-widths at half-maximum ) of the velocity distributions are summarized in Table I. It is evident, without any detailed analysis, that the spectra display a normal kinematic shift, i.e. fragments emitted at forward angles have higher mean energies than those emitted at backward angles. This result appears to rule out the possibility that the backward enhancement in the angular distribution could be due to the breakup of a nucleus moving in a direction opposite to that of the beam.

B. Two-step vector model analysis

In order to obtain further insight into the nature of the mechanism responsible for the formation of Sc fragments, the results may be analyzed in terms of the two-step vector model commonly used to interpret high-energy reactions. The velocity $\vec{v}_L$ of a particular recoil in the laboratory system is expressed as the vector sum of two velocities, $\vec{v}_L = \vec{v} + \vec{V}$. The velocity $\vec{v}$ is that acquired by the struck nucleus as a result of the initial proton-nucleus interaction while $\vec{V}$ is the velocity acquired by the fragment as a result of breakup. The vector $\vec{v}$ has components along and perpendicular to the beam direction designated $v_{||}$ and $v_{\perp}$, respectively. The model requires that the two steps of the reaction be sufficiently well separated in time so that the memory of the beam direction (except for

angular momentum effects) is lost at the time of breakup. As a result, the angular distribution of $\vec{V}$ in the moving system must, on the average, be symmetric about 90° to the beam direction. It is convenient to define the velocity ratios $\eta_{||} = v_{||}/V$ and $\eta_{\perp} = v_{\perp}/V$.

The mean value of the parallel component of the impact velocity $\langle v_{||} \rangle$ may be obtained from the spectra obtained at forward and backward angles by the relation

$$\langle v_{||} \rangle = (\langle v_F \rangle^2 - \langle v_B \rangle^2) \; / \; [2(\langle v_F \rangle \cos \theta_F - \langle v_B \rangle \cos \theta_B)] \quad (1)$$

where $\langle v_F \rangle$ is the mean laboratory velocity observed at forward angle $\theta_F$ and $\langle v_B \rangle$ is the corresponding velocity at backward angle $\theta_B$. Strictly speaking, $\langle v_{||} \rangle$ should be obtained by averaging over all velocities at all angles but the above approximation is perfectly adequate for our purpose. Similarly, $\langle V \rangle$ may be obtained from the spectra by the relation

$$\langle V \rangle^2 = \langle v_L \rangle^2 + \langle v_{||} \rangle^2 - 2 \langle v_L \rangle \langle v_{||} \rangle \cos \theta_L \quad (2)$$

Eqs. (1) and (2) are coupled in the sense that the forward and backward angles used to derive $\langle v_{||} \rangle$ necessarily yield the same value of $\langle V \rangle$. An independent result, designated $\langle V \rangle_{90}$, may be derived from the 90° spectra. However, this value includes a contribution from $v_{\perp}$.

The results of this analysis are summarized in Table II. As expected, the values of $\langle v_{||} \rangle$ are positive and their magnitude corresponds to $\beta \sim 0.003$. The values of $\langle v_{||} \rangle$ may be combined with those of $\langle V \rangle$ to obtain the corresponding mean velocity ratios, designated $\langle \eta_{||} \rangle_R$, and the latter are tabulated. Essentially comparable $\eta_{||}$ may be obtained from the angular distributions by means of a vector-model analysis in which

the laboratory curves are transformed to a system symmetrizing the distributions. We neglect, without significant error, the very slight difference between these two types of $\eta_{||}$ resulting from the differences in averaging entailed in their evaluation.[8] The results, taken from our angular distribution study,[11] are designated $\langle\eta_{||}\rangle_\theta$ and summarized in Table II. If the reaction leading to the formation of Sc nuclides involved a two-step process, the two sets of $\langle\eta_{||}\rangle$ should be equal to each other. It may be noted, however, that not only do $\langle\eta_{||}\rangle_R$ and $\langle\eta_{||}\rangle_\theta$ differ in magnitude, but even more fundamentally, they differ in sign. The forward and backward spectra thus show that the struck nucleus moves along the beam direction while the angular distributions indicate that it moves in the opposite direction. The discrepancy is a clear indication that the reaction is inconsistent with the occurrence of two distinct and temporally well separated steps.

In reaching this conclusion we have so far not considered the effect of possible correlations between $v_{||}$ and V. Cumming and collaborators[8,9,19] have explored the effect of these correlations and found that they can indeed change the conclusions based on experiments of the present type. For instance, a positive correlation between $v_{||}$ and V will result in $\langle\eta_{||}\rangle_\theta$ being smaller in magnitude than $\langle\eta_{||}\rangle_R$ while a negative correlation has the opposite effect. Correlations do not, however, lead to $\langle\eta_{||}\rangle$ of opposite sign and so cannot account for the observed results.

We have so far not considered the effect of a transverse component of the impact velocity on the results of the above analysis. The effect of $v_\perp$ is most clearly seen in the 90° spectra. When $v_\perp$ is rela-

tively large, the 90° spectra are broader than those determined at forward and backward angles. In addition, $\langle V \rangle_{90}$ will be larger than $\langle V \rangle$. The data in Table I indicate that the widths of the 90° spectra are comparable to those of the other spectra, while Table II shows that, within the limits of error, the values of $\langle V \rangle$ and $\langle V \rangle_{90}$ are equal. We conclude from these observations that $\langle v_\perp \rangle$ must be small, probably no larger than $\langle v_\parallel \rangle$. Cumming[8,9] has shown that such small $\langle v_\perp \rangle$ have a negligible effect on the transformation of the angular distribution from the laboratory to the moving system or vice-versa.

The above conclusions regarding the applicability of the two-step model thus hold up even when various refinements in the analysis are considered. While such a mechanism can thus be ruled out, the spectra are nonetheless suggestive of a modified two-step process in which a memory of the beam direction is still retained at the time the second step occurs. However, the moving system can in this case no longer be uniquely defined. One particularly appropriate system is the one moving in the laboratory with velocity $v_\parallel$ as derived from the spectra, and thus leading to the same mean breakup velocity at all angles. The laboratory angular distributions may be transformed to this system by means of standard relationships.[26] As an example of this procedure, Fig. 4 shows the angular distribution of $^{47}$Sc in the laboratory system[11] and in the system moving with $v_\parallel = 0.086$ $(\text{MeV/A})^{1/2}$. It is seen that the backward enhancement in the moving system is even more pronounced than it is in the laboratory. The F/B ratios in the laboratory and moving systems thus are 0.92 and 0.81, respectively. Evidently, fragment emission at forward angles is hindered.

C. Angular distribution of energy-selected fragments

The conclusions derived from the vector-model analysis were obtained by averaging the spectra over all velocities. Additional information may be obtained from an examination of the angular distribution of fragments having different energies. This type of analysis is commonly used in low-energy nuclear reactions, where it has generally been found that the angular distribution of energetic particles is strongly forward-peaked while that of low-energy particles is fairly symmetric. This is usually taken as evidence that the most energetic particles result from a direct process while the low-energy particles are evaporated from an equilibrated nucleus. For the purposes of the present analysis we have divided the fragments into 20 MeV wide bins covering the 10-150 MeV energy interval. The relative number of fragments in each group was determined for the 17°, 90°, and 163° spectra after the latter had been adjusted in relative intensity on the basis of the previously determined angular distributions.[11] In short, a three point laboratory angular distribution was generated for the different energy Sc fragments. Since the spectra and angular distributions of the various isotopes are virtually identical, the data were averaged over mass number in order to reduce the statistical uncertainties.

The resulting angular distributions are displayed in Fig. 5, where in each case the differential cross sections are normalized to unity at 90°. In our previous angular distribution study of Sc fragments[11] we found that the differential cross sections were well described by the function $1 + A_1 \cos \theta_L + A2 \cos^2\theta_L$, where $\theta_L$ is the laboratory angle

and $A_1$ and $A_2$ are constants whose values determine the shape of the curve. We have assumed that the angular distributions of energy-selected fragments could also be described by this function and the results of this parametrization are given by the curves in Fig. 5. The values of $A_1$ and $A_2$ are uniquely determined by the data and their dependence on fragment energy is displayed in Fig. 6. Also included in Fig. 6 are the values of F/B obtained by integrating the parametrized angular distributions over the forward and backward hemispheres.

The results display some interesting and perhaps unexpected trends. It is thus seen that backward enhancement is most pronounced for the lowest-energy fragments, for which $A_1 \sim -0.3$ and $F/B \sim 0.7$. The parameter $A_1$ increases linearly with fragment energy and changes sign in the vicinity of 70 MeV. This trend is so pronounced that the angular distribution of the lowest energy fragments appears to peak at backward angles while that of the highest energy fragments is consistent with forward peaking. The parameter $A_2$, which is a measure of the anisotropy, is negative at all energies indicating the importance of sideward relative to forward-backward emission. It appears that $A_2$ becomes increasingly negative with increasing fragment energy up to perhaps 100 MeV, at which point it levels off or maybe even decreases. Note, however, that the variation with fragment energy of $A_2$ is much less pronounced than that of $A_1$, so that the changes in the forward-backward asymmetry dominate the behavior of the angular distributions.

Although previous experiments of the present type have not been analyzed in this manner the results reported in the literature permit

at least a semiquantitative analysis to be performed. We have thus examined the results reported for the formation of $^{131}$Ba from the interaction of $^{238}$U with 2.2 GeV protons[9], a reaction that was found to be consistent with the two-step model. It appears that in this case the angular distribution of all $^{131}$Ba fragments is forward-peaked, with the forward-backward asymmetry increasing with fragment energy. The same result is obtained from the data reported for the formation of $^{24}$Na in the interaction of $^{209}$Bi with 2.9 GeV protons[8], although there is an indication that the lowest energy fragments have an angular distribution peaking at sideward angles. The present results for the low-energy Sc fragments are thus unique in displaying strongly enhanced emission at backward angles. On the other hand, the higher energy Sc fragments have an angular distribution that is more akin to those of other deep spallation and fragmentation products that have been studied in this fashion. None of the experiments appear to yield the trend expected for a two-step process involving no correlations between $\langle v_{||} \rangle$ and $\langle V \rangle$, i.e. an inverse dependence of the forward peaking on fragment energy.

## IV. Conclusions

The energy spectra of Sc fragments emitted at forward and backward angles to the beam in the interaction of $^{238}$U with 400 GeV protons, together with the fragment angular distributions, permit a test of the two-step model of high-energy reactions. The spectra are shifted to higher energies at forward angles, indicating that the struck nucleus moves in the forward direction with a mean velocity $\langle v_{||} \rangle = 0.100 \pm 0.013$ (MeV/A)$^{1/2}$, corresponding to $\beta \sim 0.003$. When the angular distribution is transformed to a system moving with this velocity the resulting curve is not symmetric about 90°, indicating that the impact and breakup steps

are not temporally well separated. It is found, instead, that fragments are preferentially emitted at backward angles in this moving system. This conclusion is not affected by possible correlations between the impact and breakup velocities or by the inclusion in the analysis of the small transverse component of the impact velocity that may be inferred from the data. A detailed inspection of the laboratory angular distributions of energy selected fragments indicates that the lowest energy fragments show strong preferential emission at backward angles. Intermediate energy fragments have nearly symmetric angular distributions exhibiting strong sideward peaking, while the highest energy fragments are preferentially emitted at forward angles.

Although several previous experiments of the present type have also yielded results inconsistent with the two-step model,[8,20,21] the angular distributions were invariably found to be forward peaked in the moving system. The present study provides the first example of a fragment angular distribution displaying a preferential enhancement at backward angles in the moving system. This result may be a consequence of the extensive mass dissipation that appears to precede the formation of Sc fragments at 400 GeV.[7] According to the coherent interaction model, the initial proton-nucleus interaction ejects an imaginary longitudinal tube of excited hadronic matter from the nucleus along the beam direction. Additional mass loss from the surface of the resulting "tunnel" due to frictional effects, final state interactions, etc. would then result in a cone-shaped region of reduced nuclear density opening at forward angles. If the nucleus were to break up prior to readjustment, frag-

ment emission at forward angles would be hindered. While this explanation may have some merit, more detailed experiments are clearly needed before any definitive conclusions can be drawn. It would thus be of interest to determine whether the emission of these fragments is indeed accompanied by extensive nucleon or light particle emission at forward angles.

## Acknowledgements

This work was performed in conjunction with similar experiments by a group from the University of Chicago and we wish to acknowledge the cooperation of N. Sugarman and R. A. Johns. We are grateful to the Plastic Products and Resins Department of Du Pont for providing us with the thin Mylar foil. This work was financially supported by the U.S. Department of Energy.

## References


1. K. Beg and N.T. Porile, Phys, Rev. C3, 1631 (1971).
2. S.B. Kaufman and M.W. Weisfield, Phys. Rev. C11, 1258 (1975).
3. Ø. Scheidemann and N.T. Porile, Phys. Rev. C14, 1534 (1976).
4. S.B. Kaufman, E.P. Steinberg, and M.W. Weisfield, Phys. Rev. C18, 1349 (1978).
5. S. Biswas and N.T. Porile, Phys. Rev. C20, 1467 (1979).
6. N.T. Porile, S. Pandian, H. Klonk, C.R. Rudy, and E.P. Steinberg, Phys. Rev. C19, 1832 (1979).
7. D.R. Fortney and N.T. Porile, Phys. Rev. C21, 664 (1980).
8. J.B. Cumming, R.J. Cross, J. Hudis, and A.M. Poskanzer, Phys. Rev. 134, B167 (1964).
9. V.P. Crespo, J.B. Cumming, and A.M. Poskanzer, Phys. Rev. 174, 1455 (1978).
10. D.R. Fortney and N.T. Porile, Phys. Lett. 76B, 553 (1978).
11. D.R. Fortney and N.T. Porile, Phys. Rev. C (in press).
12. L.P. Remsberg and D.G. Perry, Phys. Rev. Lett. 35, 361 (1975).
13. N.T. Porile, D.R. Fortney, S. Pandian, R.A. Johns, T. Kaiser, K. Wielgoz, T.S.K. Chang, N. Sugarman, J.A. Urbon, D.J. Henderson, S.B. Kaufman, and E.P. Steinberg, Phys. Rev. Lett. 43, 918 (1979).
14. J.A. Urbon, S.B. Kaufman, D.J. Henderson, and E. P. Steinberg, Phys. Rev. C21, 1048 (1980).
15. N.T. Porile, Phys. Rev. 120, 572 (1960).
16. G. Berlad, A.Dar, and G. Eilam, Phys. Rev. D13, 161 (1976); Meng Ta-chung, Phys. Rev. D15, 197 (1977).
17. B.D. Wilkins, S.B. Kaufman, E.P. Steinberg, J.A. Urbon, and D.J. Henderson, Phys. Rev. Lett. 43, 1080 (1979).

18. J.B. Cumming, Phys. Rev. Lett. 44, 17 (1980).

19. V.P. Crespo, J.B. Cumming, and J.M. Alexander, Phys. Rev. C2, 1777 (1970).

20. A.M. Poskanzer, G.W. Butler, and E.K. Hyde, Phys. Rev. C3, 882 (1971).

21. G.D. Westfall, R.G. Sextro, A.M. Poskanzer, A.M. Zebelman, G.W. Butler, and E.K. Hyde, Phys. Rev. C17, 1368 (1978).

22. C.R. Rudy, N.T. Porile, and S.B. Kaufman, Nucl. Instr. Methods 138, 19 (1976).

23. D.R. Fortney, Ph.D. Thesis, Purdue University, May 1979 (unpublished).

24. L.C. Northcliffe and R.F. Schilling, Nucl.Data A7, 233 (1970).

25. J. Lindhard, M.Scharff, and M.E. Schiøtt, Kgl. Danske Videnskab. Selskab, Mat. Fys. Medd. 33, No. 14 (1963).

26. J.B. Marion, T.I.Arnette, and H.C. Owens, Oak Ridge National Laboratory Report ORNL 2574, 1959 (unpublished).

Table I. Mean energies and velocities of Sc fragments from the interaction of $^{238}U$ with 400 GeV protons.

| Angle | Nuclide | $\langle T_R \rangle$ (MeV) | $\langle v_L \rangle$ $(MeV/A)^{1/2}$ | $v_L$ width[a] $(MeV/A)^{1/2}$ |
|---|---|---|---|---|
| 17° | $^{44}Sc^m$ | 53.0±3.9 | 1.680±0.048 | 1.054±0.021 |
| | $^{46}Sc$ | 56.3±2.1 | 1.668±0.036 | 1.000±0.020 |
| | $^{47}Sc$ | 53.3±1.2 | 1.608±0.032 | 0.927±0.039 |
| | $^{48}Sc$ | 58.6±4.5 | 1.676±0.062 | 0.874±0.054 |
| | Average | 54.2±1.0 | 1.647±0.020 | 1.005±0.030 |
| 90° | $^{44}Sc^m$ | 49.2±1.2 | 1.608±0.032 | 1.038±0.020 |
| | $^{46}Sc$ | 51.3±1.9 | 1.609±0.032 | 1.002±0.118 |
| | $^{47}Sc$ | 50.6±1.0 | 1.559±0.030 | 0.979±0.027 |
| | $^{48}Sc$ | 50.4±1.0 | 1.548±0.030 | 0.966±0.022 |
| | Average | 50.3±0.6 | 1.579±0.016 | 0.999±0.019 |
| 163° | $^{44}Sc^m$ | 39.8±1.4 | 1.460±0.028 | 1.085±0.036 |
| | $^{46}Sc$ | 42.4±1.0 | 1.456±0.028 | 1.025±0.020 |
| | $^{47}Sc$ | 42.5±1.0 | 1.444±0.028 | 1.000±0.020 |
| | $^{48}Sc$ | 45.4±3.3 | 1.476±0.052 | 1.030±0.020 |
| | Average | 42.0±0.7 | 1.455±0.015 | 1.024±0.013 |

a. Full width at half-maximum

Table II. Two-step vector model analysis of spectra

| Nuclide | $\langle v_{\|\|} \rangle$ $(MeV/A)^{1/2}$ | $\langle V \rangle$ $(MeV/A)^{1/2}$ | $\langle V \rangle_{90}$ $(MeV/A)^{1/2}$ | $\langle \eta_{\|\|} \rangle_R$ | $\langle \eta_{\|\|} \rangle_\theta$ |
|---|---|---|---|---|---|
| $^{44}Sc^m$ | 0.115±0.029 | 1.570±0.056 | 1.612±0.043 | 0.073±0.019 | -0.057±0.008[a] |
| $^{46}Sc$ | 0.111±0.024 | 1.562±0.043 | 1.613±0.040 | 0.071±0.016 | -0.030±0.007 |
| $^{47}Sc$ | 0.086±0.022 | 1.526±0.039 | 1.561±0.037 | 0.056±0.014 | -0.040±0.008 |
| $^{48}Sc$ | 0.104±0.042 | 1.577±0.074 | 1.552±0.052 | 0.066±0.027 | -0.036±0.008 |
| Average | 0.100±0.013 | 1.552±0.024 | 1.582±0.021 | 0.0644±0.0084 | |

a. From Ref. 11

## Figures

Fig. 1. Differential ranges of Sc fragments emitted at 17° (top), 90° (middle), or 163° (bottom) to the beam in the interaction of $^{238}U$ with 400 GeV protons. The results are shown as solid histograms; the dashed lines represent the experimental uncertainities. The curves are the results of a fit described in the text. The arrows surmounting the curves correspond to the mean ranges, uncorrected for energy loss in the target.

Fig. 2. Energy spectra of $^{44}Sc^{m}$ fragments emitted at the indicated angles in the interaction of $^{238}U$ with 400 GeV protons. The curves through the replicate data points were obtained from the fits to the differential ranges as described in the text. The spectra are arbitrarily displaced from each other.

Fig. 3. Energy spectra of $^{47}Sc$ fragments. See Fig. 2 for details.

Fig. 4. Angular distribution of $^{47}Sc$ in the laboratory system (top panel) [ref. 11] and in the system chosen to symmetrize the velocity spectra (bottom). The points represent the experimental data and the solid curve is the result of a parametrization described in ref. 11.

Fig. 5. Angular distributions in the laboratory system of Sc fragments binned in the indicated 20 MeV wide energy intervals. The curves are the result of a parametrization described in the test. The data points have been averaged over fragment mass number and normalized to unity at 90°.

Fig. 6. Dependence of the angular distribution parameters $A_1$ and $A_2$, and of the ratio of forward-to-backward emissions F/B, on fragment energy.

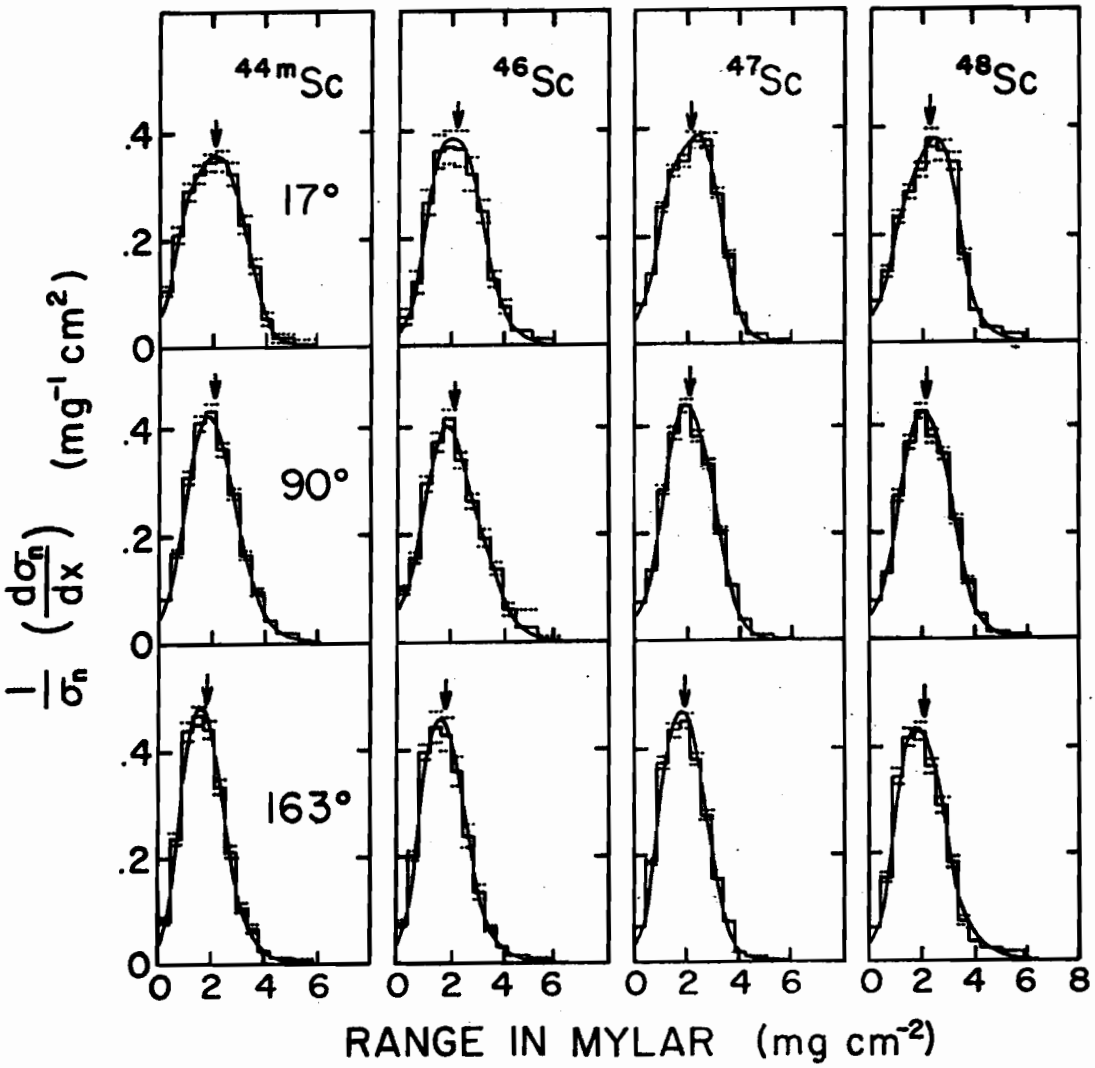
44mSc
46Sc
47Sc
48Sc
17°
90°
163°
.4
.2
0
0 2 4 6
0 2 4 6
0 2 4 6
0 2 4 6 8
$\frac{1}{\sigma_n}\left(\frac{d\sigma_n}{dx}\right)$ (mg$^{-1}$cm$^2$)
RANGE IN MYLAR (mg cm$^{-2}$)

Fig. 1

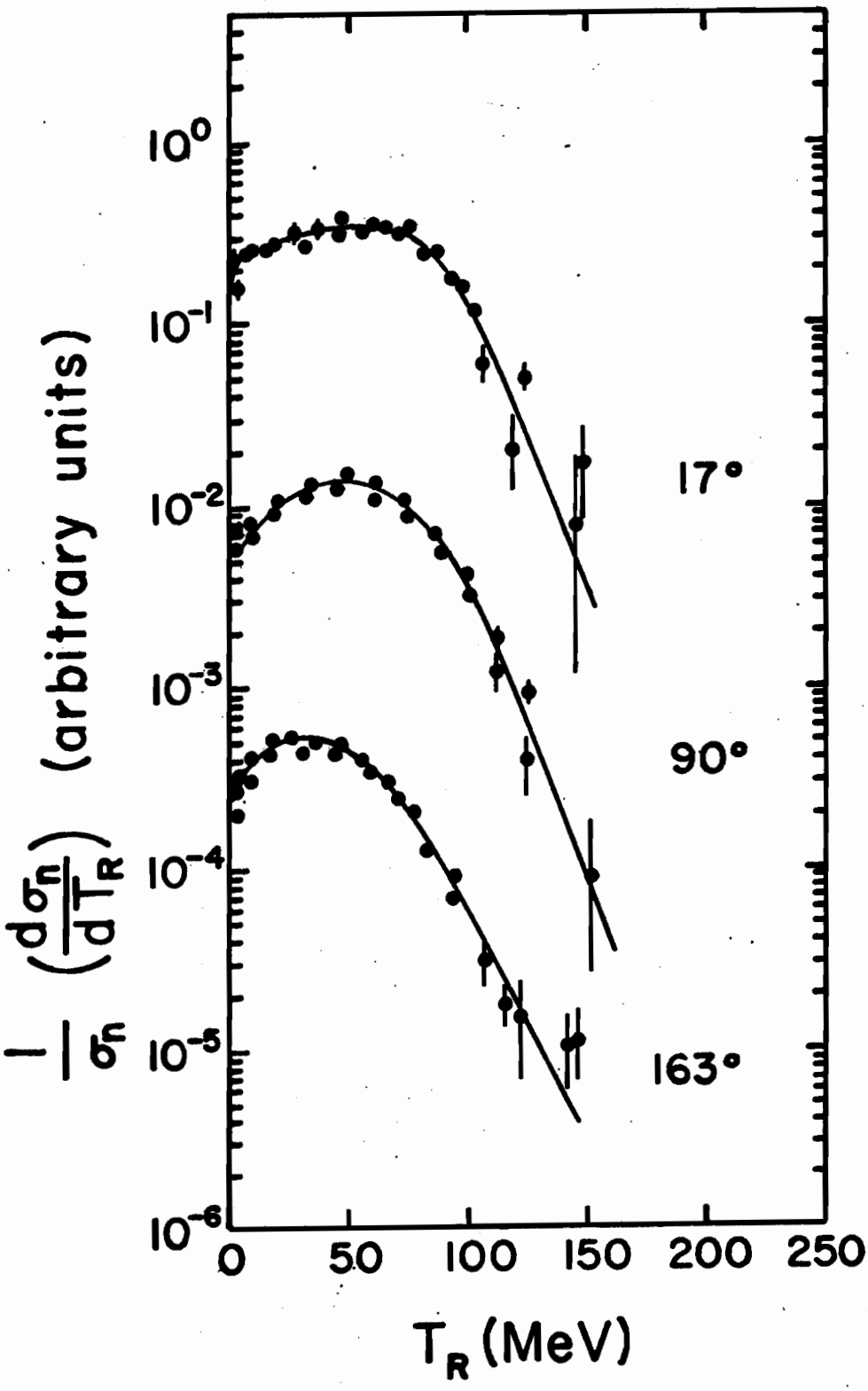
$\frac{1}{\sigma_n}\left(\frac{d\sigma_n}{dT_R}\right)$ (arbitrary units)
$10^0$
$10^{-1}$
$10^{-2}$
$10^{-3}$
$10^{-4}$
$10^{-5}$
$10^{-6}$
17°
90°
163°
0
50
100
150
200
250
$T_R$ (MeV)

Fig. 2

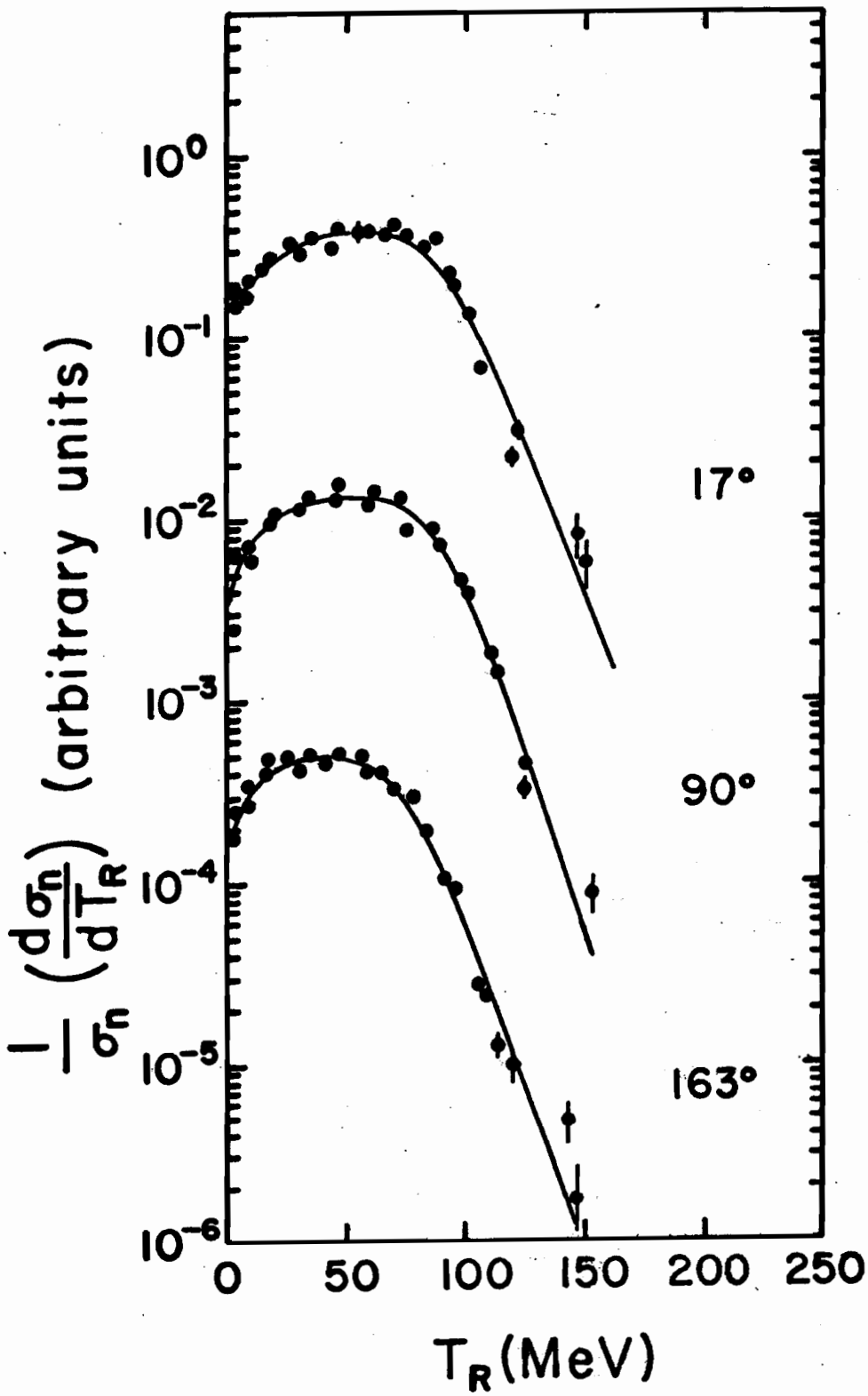
$\frac{1}{\sigma_n}\left(\frac{d\sigma_n}{dT_R}\right)$ (arbitrary units)
$10^0$
$10^{-1}$
$10^{-2}$
$10^{-3}$
$10^{-4}$
$10^{-5}$
$10^{-6}$
17°
90°
163°
0
50
100
150
200
250
$T_R$(MeV)

Fig 3

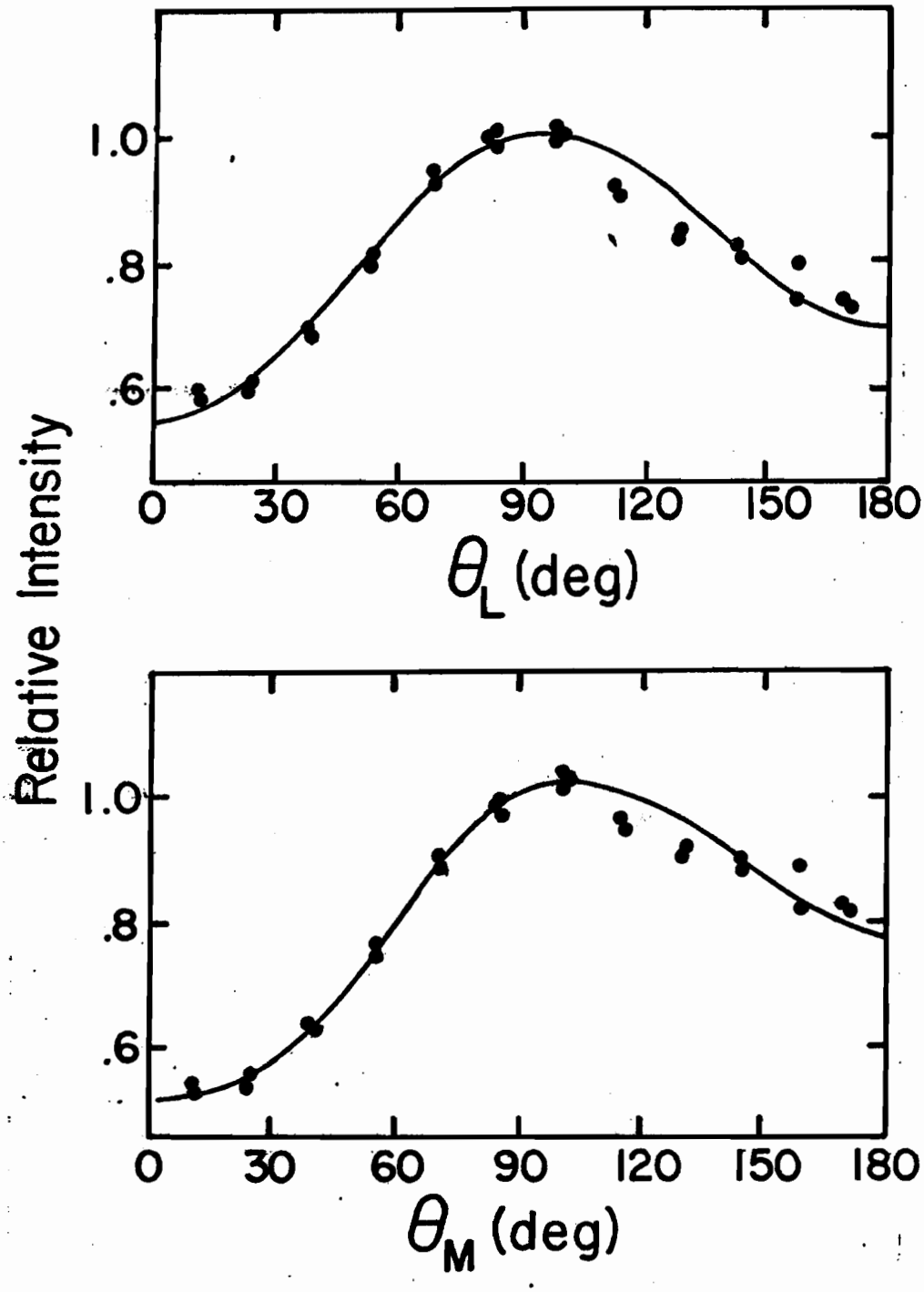


Fortney & Poole
Fig. 4

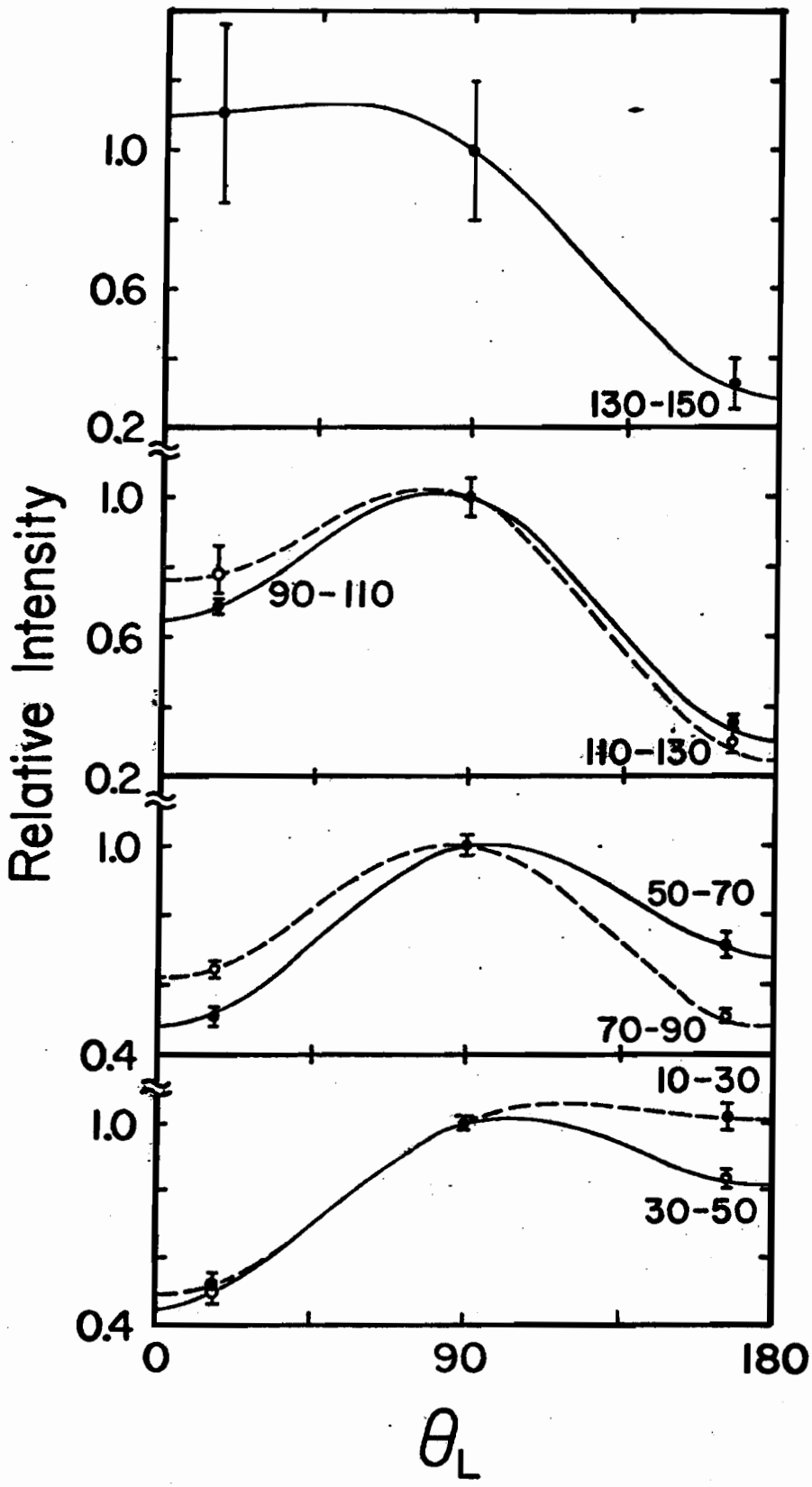


Fortney & Price
Fig. 5

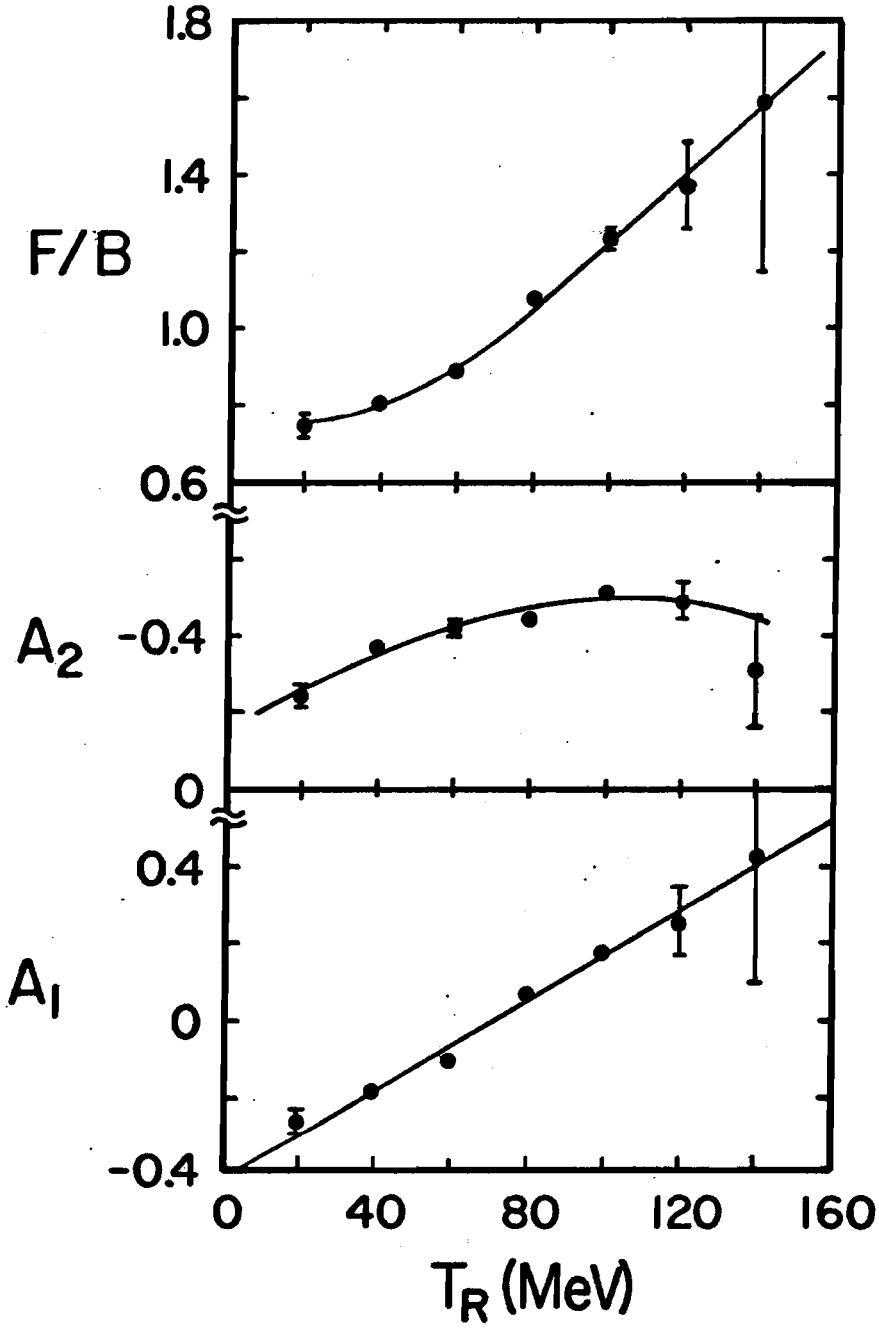


Fortney & Poirier
Fig. 6